

# Recent Progress of Lung Cancer Diagnosis Using Nanomaterials

Xuefeng Tang, Zhao Wang, Feng Wei, Wei Mu and Xiaojun Han \*

State Key Laboratory of Urban Water Resource and Environment School of Chemistry and Chemical Engineering, Harbin Institute of Technology, Harbin 150001, China; 1121430108@hit.edu.cn (X.T.); 18b902015@stu.hit.edu.cn (Z.W.); 15b925010@hit.edu.cn (F.W.); muwei@hit.edu.cn (W.M.)

\* Correspondence: hanxiaojun@hit.edu.cn

**Abstract:** Lung cancer is one of the serious malignant tumors with high morbidity and mortality due to the poor diagnosis and early metastasis. The developing nanotechnology provides novel concepts and research strategies for the lung cancer diagnosis by employing nanomaterials as diagnostic reagents to enhance diagnostic efficiency. This commentary introduces recent progress using nanoparticles for lung cancer diagnosis from two aspects of in vivo and in vitro detection. The challenges and future research perspectives are proposed at the end of the paper.

**Keywords:** nanomaterials; lung cancer diagnosis; imaging test; biomarker detection

## 1. Introduction

Environmental pollution and unhealthy living habits have caused a climbing morbidity of lung cancer. The rapid proliferation, early metastasis, low sensitivity, and poor specificity in early diagnosis cause the lung cancer the highest mortality rate among all cancers [1–3]. At present, many methods have been developed to diagnose lung cancers including sputum cytology, and pleural fluid cytology as well as the autofluorescence bronchoscopy (AFB), endoscopic ultrasound (EUS), endobronchial ultrasound (EBUS) and imageological examination, such as chest radiograph (CXR), computed tomography (CT) scan (computerized axial tomography (CAT) scan, low-dose helical CT scan) bone scans, positron emission tomography (PET) and magnetic resonance imaging (MRI) [4–9]. However, the detection of cancer biomarkers (such as specific proteins, nucleic acids, cells, and volatile organic compounds) in blood, urine, sputum, exhaled breath, and tissues are limited by the low detection sensitivity, poor specificity, complex operations, and low adsorptivity of gaseous molecules on solid substrates [10–13]. During the imageological examination, patients suffer from a heavy burden of cost and the risk of cumulative radiation [14]. Additionally, poor tissue penetration of ray and low specificity of photographic developer can cause false-negative results [15]. In clinical practice, X-ray chest imaging is a basic method to detect lung cancer without providing detailed images of inside information. Therefore, low dose computed tomography (LDCT) becomes a promising method for lung cancer screening with lower radiation and higher security [16–18]. These detection methods possess a bottleneck of an unsatisfactory sensitivity with sputum cytology of 66%, pleural fluid cytology of 70%, PET scan of 88%, CT scan of 55% and bone scan of 77% [19]. Therefore, it is essential to establish low-cost, sensitive, convenient, and non-invasive detection approaches for lung cancer diagnosis.

Nanomaterials have been widely applied in cancer diagnosis and treatment because of their excellent plasticity, controllable shapes and sizes, as well as adjustable thermal, magnetic, and optical properties [20–27]. The nanoparticles can be used as carriers to deliver anti-cancer drugs (such as small molecule drugs, RNA, and protein) [28–30]. Moreover, they can function as direct diagnostic agents according to their inherent properties, such as the superparamagnetic properties of Fe<sub>3</sub>O<sub>4</sub> nanoparticles [31], and the photoacoustic properties of melanin nanoparticles [32]. In addition to stabilizing drugs, functional nanoparticles can be obtained by surface modification, including specificity targeting,



**Citation:** Tang, X.; Wang, Z.; Wei, F.; Mu, W.; Han, X. Recent Progress of Lung Cancer Diagnosis Using Nanomaterials. *Crystals* **2021**, *11*, 24. <https://doi.org/10.3390/cryst11010024>

Received: 10 November 2020

Accepted: 25 December 2020

Published: 29 December 2020

**Publisher's Note:** MDPI stays neutral with regard to jurisdictional claims in published maps and institutional affiliations.



**Copyright:** © 2020 by the authors. Licensee MDPI, Basel, Switzerland. This article is an open access article distributed under the terms and conditions of the Creative Commons Attribution (CC BY) license (<https://creativecommons.org/licenses/by/4.0/>).

stimulus response, improving the detection sensitivity, and increasing the biocompatibility [14,31,33,34]. Moreover, a novel idea has been demonstrated to discriminate non-small cell lung cancer patients from healthy volunteers through exploiting the biomolecular corona that forms around nanoparticles to identify the differences of protein patterns between cancer patients and healthy subjects in blood [35]. Through the combination of nanotechnology and diagnostic targets, the novel diagnostic strategies with high efficiency and specificity have been developed, which are expected to improve the detection efficiency at an early stage and monitor the development trend and accurate therapeutics in the follow-up treatment of lung cancer [36].

In the past five years, the treatment of lung cancer by employing nanomaterials was reviewed [37–41], but the relationship between lung cancer diagnosis and nanomaterials still needs to be further summarized. In this commentary, we focus on the characteristics of some dominant nanomaterials, primary functions, and improvement strategies to commensurate the progress in improving detection specificity, diagnosis accuracy and internalization efficiency, when using nanomaterials in the early-stage diagnosis of lung cancer from *in vivo* detection (imageological examination) and *in vitro* detection (biomarker detection). Besides, the current challenges and the future development prospects of nanomaterials in the diagnosis of lung cancer are also discussed.

## 2. Applications of Nanoparticles in Diagnosis of Cancer

The occurrence and progression of cancer are normally accompanied by a series of changes at the molecular or cellular level, which can in turn provide specific targets for effective diagnosis. Imageological examination and biomarker detection are common diagnose methods associated with the specific target in niduses.

### 2.1. *In Vivo* Examination

The *in vivo* methods mainly include AFB, EUS, CT, PET, MRI, which can reflect the disease information by visual image. The anatomical structure and boundary range of tumor can be seen clearly due to the ultrahigh resolution of MRI, but it was limited by longer imaging time and the lack of molecular imaging information. Although PET imaging showed high sensitivity and provided systemic lesions information, it is still limited by insufficient spatial resolution and possible false positive caused by unsatisfactory specificity. Low dose CT-scans provides information to indicate size, shape, and position of cancer cells in lymph nodes, but it has the disadvantages of low sensitivity and low specificity due to severe artifacts in pictures caused by internal organ motion and tattoos.

#### 2.1.1. Single-Modal Imageological Examination-MRI

MRI is a high resolution and large-scale imaging technique facilitating the tumor observation of anatomical structures and subtle features. Nevertheless, MRI cannot yet be directly applied in the lung detection due to the motion artifacts, numerous susceptibility gradients, and low proton density [42]. By combining with the optimized proton MRI sequences based on ultrashort echo time (UTE), ultrashort echo-time magnetic resonance imaging (UTE-MRI) can be applied in lung tissue imaging [43]. Gadolinium is clinically used as the MRI contrast material, showing that non-invasive detection of non-small cell lung cancer by UTE-MRI can be achieved via the orotracheal administration of nebulized gadolinium nanoparticles with enhanced signal. Moreover, Gadolinium can be selectively deposited in tumor tissues while removed by healthy tissues [44].

Accurate and detailed detection information can be obtained through simultaneous usage of two MRI contrast agents [45–47]. MRI contrast agents can be divided into longitudinal relaxation contrast medium (T1 contrast medium, such as Gd-DTPA, Mn-DPDP) and transverse relaxation contrast medium (T2 contrast medium, such as superparamagnetic iron oxide), among which T1 contrast medium can effectively decrease the T1 relaxation time by the interactions with the neighboring T2 contrast medium [48]. The strong magnetic coupling between T1 and T2 contrast medium could disturb the relaxation effect of the

paramagnetic T1 contrast medium, leading to an undesirable weakening and quenching of magnetic resonance signal [49]. According to this, a smart MRI contrast agent with  $\text{Fe}_3\text{O}_4$  nanoparticles in core (T2 contrast medium) and the silica shell containing water-soluble Mn-porphyrin (T1 contrast medium) and anticancer drug DOX in shell was constructed (Figure 1a). After the modification by poly (acrylic acid) (PAA) and c(RGDyK) peptides (cRGD), the dual-mode MRI contrast medium was equipped with functions of tumor-specific target and pH response (Figure 1b). When the contrast medium was internalized by cancer cells, the tumor acidic microenvironment facilitated the release of porphyrin and recovered the quenched signal caused by the combination of  $\text{Fe}_3\text{O}_4$  and Mn-porphyrin (Figure 1a) [31].

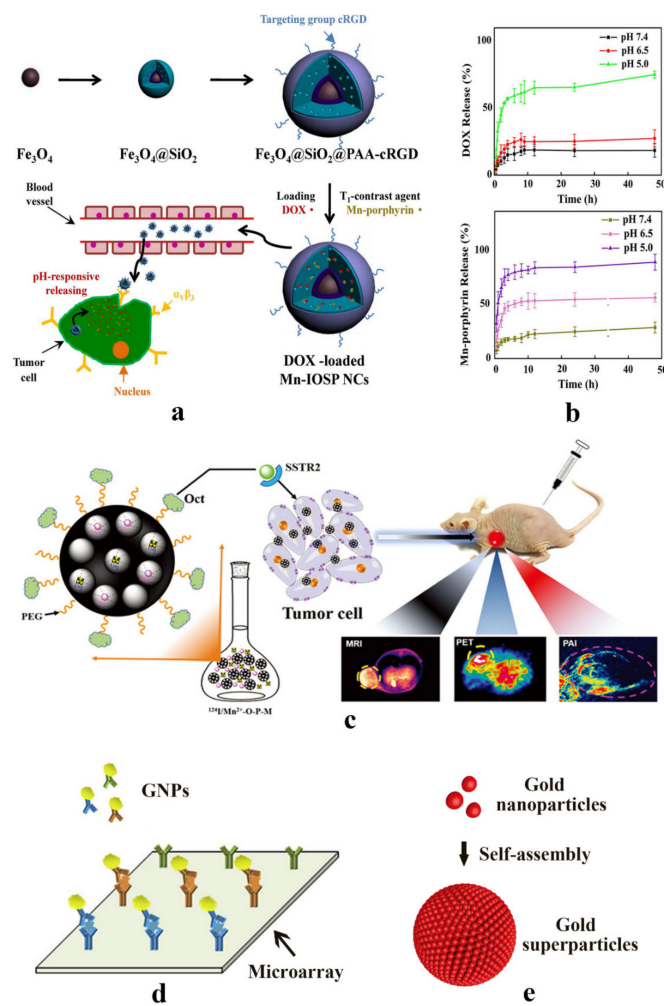


**Figure 1.** (a) Schematic illustration for the preparation, release, and imaging process of  $\text{Fe}_3\text{O}_4@SiO_2@PAA-cRGD$  as dual-mode MRI contrast medium. Reprinted from [31] with permission by Creative Commons License. (b) UV-Vis spectra analysis of drug release: a pH-dependent drug release of DOX and Mn-porphyrin in the nanoparticles in different physiological environments Reprinted from [31] with permission by Creative Commons License. (c) Schematic illustration for the contrast agent preparation and imaging mode of MRI/PET/PAI multi-modal imaging. This contrast agent can internalize by tumor cell specifically due to the interaction between Oct and SSTR2 surface receptors highly expressed in tumor cells. Reproduction from Ref. [32] with permission from The Royal Society of Chemistry. (d) The gold nanoparticles that modified by various antibodies on the surface combine with microarray for detecting various biomarkers simultaneously. Reprinted from Ref. [50] with permission from Elsevier. (e) The gold nanoparticles were constituted into gold superparticles (GSPs) by self-assembly to amplify the detection signal. Reprinted from [51] with permission of Wiley.

### 2.1.2. Single-Modal Imageological Examination-PET

PET is a diagnosis imaging technology with high sensitivity, temporal resolution, systemic image quantitative analysis, and unlimited tissue penetration [52,53]. Radio isotope used in PET imaging possesses a short half-life with  $^{11}\text{C}$  of 20 mins,  $^{13}\text{N}$  of 10 mins and  $^{15}\text{O}$  of 2 mins.  $^{64}\text{Cu}$  was widely studied due to its half-life up to 12.7 h. Researchers found that polyglucose nanoparticles consisting of cross linked dextrans and their derivatives (dextran nanoparticles) had noteworthy affinity to tumor associated macrophages (TAMs) [54,55].  $^{64}\text{Cu}$ -labeled dextran nanoparticles by macrocyclic chelators can be applied in PET imaging for clinical oncologic diagnosis. However, the poor stability of radiometal-chelator complexes in vivo [56] greatly influenced the physicochemical properties of nanoparticles in PET imaging. Hence, the chelator-free  $^{64}\text{Cu}$  nanoclusters were developed through a simple one-pot chemical reduction method by employing bovine serum albumin (BSA) as a framework for PET lung cancer detection to improve the stability and accumulation [57]. Although Cu-based radionuclide has been studied extensively and made some progress, the blemishes of its instability and higher accumulation in the liver are still the focus of lung diagnosis studies in the future.

### 2.1.3. Multi-Modal Imageological Examination

Compared to single-contrast medium imaging, multi-modal imaging with several contrast mediums can provide complementary imaging information for cancer diagnosis. Co-delivery of various contrast mediums without the imaging signal interference is a great challenge. USRPs-Cy5.5 was constructed by covalently conjugating cyanine 5.5 on nebulized gadolinium nanoparticles for fluorescence tomography and ultrashort echo-time magnetic resonance imaging (UTE-MRI) to detect lung cancer non-invasively [58]. Melanin nanoparticles photoacoustic imaging (PAI) can be used as nanocarriers to co-deliver  $^{124}\text{I}$  (PET contrast agent) and  $\text{Mn}^{2+}$  (MRI contrast agent) by an electrophilic substitution reaction and a chelation reaction respectively, which is an ideal vector for tri-mode imaging (Figure 1c) to improve the efficiency of lung cancer diagnosis at an early stage effectively [32].

### 2.2. In Vitro Detection

Biomarker testing has been demonstrated as an effective method to analyze and diagnosis cancer, including proteins (carcinoembryonic antigen (CEA), cytokeratin 19 fragment antigen 21-1 (CYFRA21-1), neuron specific enolase (NSE), dickkopf-1 (DKK1), etc.), nucleic acids (DNA, RNA), cells (TAMs), and volatile organic compounds (aldehydes) [51,59–65]. The detection of biomarker allows for serial sampling by a non-invasive way, but unsatisfactory specificity ascribe the vast inter-tumor heterogeneity [66,67]. The use of nanoparticles can enhance the sensitivity and specificity prominently (Table 1).

**Table 1.** Nanoparticles for lung cancer biomarker detection.

Nanoparticles	Cancer Biomarkers	Limit of Detection (LOD)	Methods	Ref.
Gold nanoparticles	EGFR, CK, Nap	—	Fluorescence and surface enhanced Raman scattering	[68]
	CEA, CYFRA21-1, NSE, Dkk1	<1000 pg/mL	Co-detection method based on NPs and microarrays	[50]
	MiR-205	—	Localized surface plasmon resonance	[51]
	MUC1	8 cells/mL	Chronoamperometry	[33]
	Aldehydes	10 ppb	Surface enhanced Raman scattering	[69]
Quantum dots	CEA, CYFRA21-1, NSE	CEA: 190 pg/mL; CYFRA21-1: 970 pg/mL; NSE: 370 pg/mL	Microarray immunoassay (bead bases sandwich assay)	[70]
	CYFRA21-1	0.3 pg/mL	Electrochemiluminescent immunoassay	[71]

Table 1. Cont.

Nanoparticles	Cancer Biomarkers	Limit of Detection (LOD)	Methods	Ref.
	HER2	—	Western Blot, ELISA, confocal microscopy, flow cytometry	[72]
Carbon nanomaterials	CEA/EGFR	14 cells/mL	Differential pulse voltammetry	[73]
Liposome	TKTL1, TTF1	—	TIRF and TLN biochip	[15]
Fe <sup>0</sup> nanomaterials	ctDNA	0.1 pg/mL	Inductively coupled plasma mass spectrometry	[62]
Fluorescent nanoparticles	EGFR	—	Western Blot, confocal microscopy, flow cytometry	[14]
Fe <sub>3</sub> O <sub>4</sub> /Au/Ag nanocomposites	Adenosine	—	Surface enhanced Raman scattering	[74]

### 2.2.1. Gold Nanoparticles

Gold nanoparticles have been extensively used for cancer biomarker detection owing to the surface plasmon resonance (SPR) effect, controllable particle volume and size, and excellent biocompatibility. SPR effect was used to generate and magnify the detection signal. The mucin 1 (MUC1) specific aptamer [75,76] was covalently conjugated with gold nanoparticles through the self-assembly of 4-([2,2':5',2''-terthiophen]-3'-yl) benzoic acid (TTBA). This ultrasensitive cytosensing can prominently amplify the selective detection signal of lung cancer with the detection limit of 8 cells/mL [33]. In order to control the detection process, an enzyme was added to trigger the detection. The gold nanoparticles were linked with dual-functional Raman active luciferin by a peptide linker, and the peptide linker was engineered with a cathepsin B enzyme (CathB) cleavage site. Assisted by these antibodies (epidermal growth factor receptor (EGFR), cytokeratin-19 (CK), and napsin-A (Nap)) and CathB enzyme *in vivo*, the nanoprobe is endowed with multi-target to lung cancer and enzyme-driven fluorescence imaging [68]. The gold nanocubes can be used to test infinitesimal lung cancer biomarker miR-205 after modified by thiolated single strand DNA (ssDNA), which can realize real-time monitoring of the slight LSPR scattering peak displacement caused by the hybridization process of target miRNA with ssDNA [51]. In order to improve the detection sensitivity, two nanoparticles were combined for the detection of circulating tumor DNA (ctDNA). The amorphous Fe<sup>0</sup> nanomaterials are featured with excellent magnetic performances and high monodispersity, which allows the separation and enrichment of the subtle ctDNA, and the Au nanoparticles enables the prominent amplifying detection signal. Taking the detection of Kirsten rat sarcoma-2 virus (KRAS) mutation as an example, 0.1 pg/mL gene mutation can be detected by Fe–Au nanoparticle, which refers to the stage I diagnosis. This method avoided the test deviation caused by the amplification of traditional PCR [62].

Assisted with microarray technology, gold nanoparticles conjugated to detection antibodies on microarrays can further enhance the amplifying detection signal through immersing in a solution of H<sub>2</sub>O<sub>2</sub> and H<sub>2</sub>SO<sub>4</sub>, which can be used to detect four kinds of markers (CEA, CYFRA21-1, NSE, DKK1) at the same time (Figure 1d) [50]. The gold nanoparticles can constitute gold superparticles (GSPs) through self-assembly to amplify the Raman signal (Figure 1e) [51]. Despite their ultrahigh sensitivity for lung cancer noninvasive diagnosis *in vitro*, the potential toxicity of nanoparticles needs to be addressed [69].

### 2.2.2. Quantum Dots (QDs)

QDs were often used to establish electrochemical luminescence (ECL) sensor due to its high fluorescence intensity, unique size-dependent electrochemical properties, long fluorescence lifetime, strong photostability, and ECL parameter tenability [77–80]. The detection limit based on QDs (0.3 pg/mL) was much lower than that of other detection

method (0.65 pg/mL) [71]. A suspension and planar microarray system can be set up based on the low cost and high throughput detection of multiple markers (CEA, CYFRA21-1, NSE). Briefly, the suspension state was ground on the target proteins to constitute a sandwich structure between the magnetic beads and the QDs through specific antibody–antigen interactions [70]. Inherently, the modification of lung cancer-specific antibody on the surface of QDs can realize the target detection theoretically. Undesirable issues came up for practical applications, such as decreasing the detection sensitivity for intracellular tumor biomarker due to the larger complexes formed between QDs and antibody as well as the inactivity of the lung cancer-specific antibody engineered on the QDs surface. Fortunately, the traditional antibody can be substituted by the single domain antibody (sdAb), which can reduce the molecular weight prominently [72,81,82]. Although the surface modification of QDs can be used to improve biocompatibility to alleviate the biological toxicity to cells, the security and targeting specificity are still major obstacles that QDs face [83].

### 2.2.3. Carbon Nanomaterials

Carbon nanomaterials are potential candidates for constructing electrochemical biosensors due to the large surface area, chemical, and thermal stabilities, excellent electrical and thermal conductivity, extraordinary electron transport rate, tunable band gap, and great mechanical strength [59,84,85]. Graphene oxide and ordered mesoporous carbon can be deposited onto nano-carrier surface by two-step electropolymerization to improve electrical conductivity and electrochemical effective surface area [86]. An electrochemical cytosensor based on 3D carbon nanosphere was prepared through a microwave-hydrothermal method, and then gold nanoparticles were self-assembled on its surface to detect CEA, showing that the detection sensitivity was significantly improved and detection limit decreased to 14 cells/mL, due to the promotion of electron transfer caused by the synergism of monodisperse colloidal carbon nanospheres and gold nanoparticles [73]. Single-wall carbon nanotubes decorated by platinum-group transition metals were prepared as biosensors to enhance the detection of toluene, which was a biomarker of the lung cancer in the patients exhaled breath, and the effective detection contributed to the strong overlapping between d orbital of the metal atoms and p orbital of C atoms in the benzene ring of toluene [87].

### 2.2.4. Others

Additionally, there are some other nanomaterials that have been studied and applied to detect lung cancer biomarker. The lipid bilayer is composed of phospholipids and cholesterol, which is similar to the cell membrane [59,88–94]. Hence liposomes have higher biosafety and biocompatibility compared to other synthetic materials [95]. As the vehicles of transketolase 1 (TKTL1) and thyroid transcription factor 1 (TTF1), liposomes can capture circulating extracellular vesicles by electrostatic interaction to constitute a larger nanoscale compound and detect RNA concentration in the plasma of lung cancer patients [15]. The Fe<sub>3</sub>O<sub>4</sub>/Au/Ag nanocomposites and fluorescent nanoparticles have also been used in early diagnosis due to the magnetism assisted surface enhanced Raman scattering (SERS) effect of Fe<sub>3</sub>O<sub>4</sub>/Au/Ag nanocomposites, the advantages of highly efficient red emission, high resolution, and excellent photostability of fluorescent nanoparticles [14,74].

## 3. Cellular Uptake of Nanomaterials

Understanding the lung cancer cells internalization pathway of nanomaterials is essential to realizing the detection of lung cancer, particularly in vivo detection. Cellular uptake is a dynamic process which is determined to a great extent by physicochemical property of nanomaterials, such as size, shape, surface charge, hydrophilia/hydrophobicity, and the specific ligand [96–98]. According to the characteristics of size and shape, several common pathways for uptake mainly include phagocytosis, clathrin mediated endocytosis, receptor-mediated endocytosis, caveolae-dependent endocytosis, and membrane permeation. High specificity, low systematic side effects, and escaping from the capture of

reticuloendothelial system permit pulmonary delivery to be widely used in pulmonary disease treatment, as well as in lung cancer diagnosis. The inhalant 5  $\mu\text{m}$  in diameter can effectively deposit in the lungs, because the mission of phagocytosis is to transmit larger particles greater than 200 nm [96,99]. The nanoparticles of  $\sim 100$  nm in diameter were commonly used as tumor agents (diagnosis or imaging) and carriers because of their enhanced permeability and retention (EPR) effect in systemic delivery system. These nanoparticles internalized not only through clathrin mediated endocytosis [100], but also through receptor-mediated endocytosis after modified by lung cancer specific ligand [101]. Cellular uptake of nanoparticles about 50 nm was via caveolae-dependent endocytosis, but these particles were not suitable for lung cancer detection due to the cumulation in liver and kidney. The 2D morphology allowed nanomaterials to enter cells and bypass the lysosome by a membrane permeation, such as black phosphorus nanosheets and 2D graphene sheet [102]. In addition, nanoparticles with moderate positive charge can easily enter cells with negative charge with the assist of electrostatic interaction, which can also contribute to intracellular escape [103,104].

#### 4. Conclusions

The challenges in application of nanomaterials for diagnosing lung cancer have been widely summarized. Although various nanoparticles have been demonstrated for detecting lung cancer and have already made significant progress in increasing detection limit, sensitivity, simplifying the detection operations, and shortening the detection time, it still needs to break through the limitations from the specificity and biosafety, detection efficiency, diagnostic cost, and patient tolerance. Nanomaterials are expected to contribute to overcoming the above challenges through increasing the internalization of diagnostic reagent into lung cancer cells instead of normal cells, or specifically binding to lung cancer biomarkers in vitro, due to the controllable sizes, shapes, physicochemical property (such as thermal, magnetic, and optical properties), and the characteristics of modifiable surfaces. Meanwhile, the combination of nanotechnology, array technology, and chip technology is a good option to surmount the barriers of inefficiency and high expenditure in lung cancer detection. The improvement of non-invasive detection methods should be paid more attention, aiming to increase the detection efficiency without additional harm. In the future, the combination of clinical diagnostic and biomedicine, nanotechnology, and material science will contribute to overcoming the current challenges in lung cancer early diagnosis.

**Author Contributions:** Conceptualization, X.T. and X.H.; software, X.T. and Z.W.; writing—original draft preparation, X.T.; writing—review and editing, X.T., Z.W., F.W., and X.H.; visualization, F.W.; supervision, F.W. and W.M.; project administration, X.H.; funding acquisition, X.H. All authors have read and agreed to the published version of the manuscript.

**Funding:** This research was funded by the National Natural Science Foundation of China (Grant No. 21773050, 21929401), and the Natural Science Foundation of Heilongjiang Province for Distinguished Young Scholars (JC2018003).

**Institutional Review Board Statement:** Not applicable.

**Informed Consent Statement:** Not applicable.

**Data Availability Statement:** Data sharing is not applicable to this article as no new data were created or analyzed in this study.

**Conflicts of Interest:** The authors declare no conflict of interest.

#### References

1. Siegel, R.L.; Miller, K.D.; Jemal, A. Cancer statistics, 2019. *CA Cancer J. Clin.* **2019**, *69*, 7–34. [[CrossRef](#)] [[PubMed](#)]
2. Silva, M.; Galeone, C.; Sverzellati, N.; Marchiano, A.; Calareso, G.; Sestini, S.; La Vecchia, C.; Sozzi, G.; Pelosi, G.; Pastorino, U. Screening with low-dose computed tomography does not improve survival of small cell lung cancer. *J. Thorac. Oncol.* **2016**, *11*, 187–193. [[CrossRef](#)] [[PubMed](#)]
3. Doroudian, M.; MacLoughlin, R.; Poynton, F.; Prina-Mello, A.; Donnelly, S.C. Nanotechnology based therapeutics for lung disease. *Thorax* **2019**, *74*, 965–976. [[CrossRef](#)] [[PubMed](#)]

4. Gould, M.K.; Donington, J.; Lynch, W.R.; Mazzone, P.J.; Midthun, D.E.; Naidich, D.P.; Wiener, R.S. Evaluation of individuals with pulmonary nodules: When is it lung cancer? Diagnosis and management of lung cancer, 3rd ed: American college of chest physicians evidence-based clinical practice guidelines. *Chest* **2013**, *143*, E93–E120. [[CrossRef](#)]
5. Lu, H.; Zhang, H.; Wei, Y.; Chen, H. Ambient mass spectrometry for the molecular diagnosis of lung cancer. *Analyst* **2020**, *145*, 313–320. [[CrossRef](#)]
6. Khanmohammadi, A.; Aghaie, A.; Vahedi, E.; Qazvini, A.; Ghanei, M.; Afkhami, A.; Hajian, A.; Bagheri, H. Electrochemical biosensors for the detection of lung cancer biomarkers: A review. *Talanta* **2020**, *206*, 120251. [[CrossRef](#)]
7. Salehi-Rad, R.; Li, R.; Paul, M.K.; Dubinett, S.M.; Liu, B. The biology of lung cancer: Development of more effective methods for prevention, diagnosis, and treatment. *Clin. Chest Med.* **2020**, *41*, 25–38. [[CrossRef](#)]
8. Nardi-Agmon, I.; Peled, N. Exhaled breath analysis for the early detection of lung cancer: Recent developments and future prospects. *Lung Cancer* **2017**, *8*, 31–38. [[CrossRef](#)]
9. Kim, I.D. How can nanotechnology be applied to sensors for breath analysis? *Nanomedicine* **2017**, *12*, 2695–2697. [[CrossRef](#)]
10. Van Cutsem, E.; Kohne, C.-H.; Lang, I.; Folprecht, G.; Nowacki, M.P.; Cascinu, S.; Shchepotin, I.; Maurel, J.; Cunningham, D.; Tejpar, S.; et al. Cetuximab plus irinotecan, fluorouracil, and leucovorin as first-line treatment for metastatic colorectal cancer: Updated analysis of overall survival according to tumor kras and braf mutation status. *J. Clin. Oncol.* **2011**, *29*, 2011–2019. [[CrossRef](#)]
11. Altelaar, A.F.M.; Munoz, J.; Heck, A.J.R. Next-Generation proteomics: Towards an integrative view of proteome dynamics. *Nat. Rev. Genet.* **2013**, *14*, 35–48. [[CrossRef](#)] [[PubMed](#)]
12. Capuano, R.; Catini, A.; Paolesse, R.; Di Natale, C. Sensors for lung cancer diagnosis. *J. Clin. Med.* **2019**, *8*. [[CrossRef](#)] [[PubMed](#)]
13. Nakhleh, M.K.; Amal, H.; Jeries, R.; Broza, Y.Y.; Aboud, M.; Gharra, A.; Ivgi, H.; Khatib, S.; Badarneh, S.; Har-Shai, L.; et al. Diagnosis and classification of 17 diseases from 1404 subjects via pattern analysis of exhaled molecules. *ACS Nano* **2017**, *11*, 112–125. [[CrossRef](#)] [[PubMed](#)]
14. Gao, M.; Su, H.; Lin, G.; Li, S.; Yu, X.; Qin, A.; Zhao, Z.; Zhang, Z.; Tang, B.Z. Targeted imaging of EGFR overexpressed cancer cells by brightly fluorescent nanoparticles conjugated with cetuximab. *Nanoscale* **2016**, *8*, 15027–15032. [[CrossRef](#)]
15. Lee, L.J.; Yang, Z.; Rahman, M.; Ma, J.; Kwak, K.J.; McElroy, J.; Shilo, K.; Goparaju, C.; Yu, L.; Rom, W.; et al. Extracellular mRNA detected by tethered lipoplex nanoparticle biochip for lung adenocarcinoma detection. *Am. J. Respir. Crit. Care. Med.* **2016**, *193*, 1431–1433. [[CrossRef](#)]
16. Tartarone, A.; Lerosé, R.; Aieta, M. Focus on lung cancer screening. *J. Thorac. Dis.* **2020**, *12*, 3815–3820. [[CrossRef](#)]
17. Saadat, M.; Manshadi, M.K.D.; Mohammadi, M.; Zare, M.J.; Zarei, M.; Kamali, R.; Sanati-Nezhad, A. Magnetic particle targeting for diagnosis and therapy of lung cancers. *J. Control. Release* **2020**, *328*, 776–791. [[CrossRef](#)]
18. Chen, K.N. The diagnosis and treatment of lung cancer presented as ground-glass nodule. *Gen. Thorac. Cardiovasc. Surg.* **2020**, *68*, 697–702. [[CrossRef](#)]
19. Mottaghtalab, F.; Farokhi, M.; Fatahi, Y.; Atyabi, F.; Dinarvand, R. New insights into designing hybrid nanoparticles for lung cancer: Diagnosis and treatment. *J. Control. Release* **2019**, *295*, 250–267. [[CrossRef](#)]
20. Cryer, A.M.; Thorley, A.J. Nanotechnology in the diagnosis and treatment of lung cancer. *Pharmacol. Ther.* **2019**, *198*, 189–205. [[CrossRef](#)]
21. Yang, C.Y.; Chen, Y.D.; Guo, W.; Gao, Y.; Song, C.Q.; Zhang, Q.; Zheng, N.N.; Han, X.J.; Guo, C.S. Bismuth ferrite-based nanoplatform design: An ablation mechanism study of solid tumor and nir-triggered photothermal/photodynamic combination cancer therapy. *Adv. Funct. Mater.* **2018**, *28*. [[CrossRef](#)]
22. Cui, X.Y.; Cheng, W.L.; Xu, W.L.; Mu, W.; Han, X.J. Functional graphene derivatives for chemotherapy-based synergistic tumor therapy. *NANO* **2019**, *14*. [[CrossRef](#)]
23. Cui, X.Y.; Cheng, W.L.; Han, X.J. Lipid bilayer modified gold nanorod@mesoporous silica nanoparticles for controlled drug delivery triggered by near-infrared light. *J. Mater. Chem.* **2018**, *6*, 8078–8084. [[CrossRef](#)] [[PubMed](#)]
24. Cui, X.Y.; Cheng, W.L.; Dong, M.D.; Han, X.J. A multifunctional biomimetic hybrid nanocarrier for the controlled delivery of chemotherapy drugs by near-infrared light. *New J. Chem.* **2019**, *43*, 2752–2757. [[CrossRef](#)]
25. Yang, C.Y.; Guo, C.S.; Guo, W.; Zhao, X.L.; Liu, S.Q.; Han, X.J. Multifunctional bismuth nanoparticles as theranostic agent for PA/CT imaging and NIR laser-driven photothermal therapy. *ACS Appl. Nano Mater.* **2018**, *1*, 820–830. [[CrossRef](#)]
26. Yang, C.Y.; Huang, W.C.; Gao, Y.; Liu, Z.; An, N.; Mu, W.; Pan, Q.M.; Yang, B.; Guo, C.S.; Han, X.J. Phototherapy ablation of rabbit orthotopic tumors by non-stoichiometric BiPO<sub>4</sub>-x nanoparticles. *Chem. Eng. J.* **2020**, *386*. [[CrossRef](#)]
27. Yang, C.Y.; Yu, H.H.; Gao, Y.; Guo, W.; Li, Z.Z.; Chen, Y.D.; Pan, Q.M.; Ren, M.; Han, X.; Guo, C.S. Surface-Engineered vanadium nitride nanosheets for an imaging-guided photothermal/photodynamic platform of cancer treatment. *Nanoscale* **2019**, *11*, 1968–1977. [[CrossRef](#)]
28. Gu, L.; Deng, Z.J.; Roy, S.; Hammond, P.T. A combination RNAi-chemotherapy layer-by-layer nanoparticle for systemic targeting of KRAS/P53 with cisplatin to treat non-small cell lung cancer. *Clin. Cancer Res.* **2017**, *23*, 7312–7323. [[CrossRef](#)]
29. Song, W.; Kuang, J.; Li, C.-X.; Zhang, M.; Zheng, D.; Zeng, X.; Liu, C.; Zhang, X.-Z. Enhanced immunotherapy based on photodynamic therapy for both primary and lung metastasis tumor eradication. *ACS Nano* **2018**, *12*, 1978–1989. [[CrossRef](#)]
30. Van Rijt, S.H.; Boeluekbas, D.A.; Argyo, C.; Datz, S.; Lindner, M.; Eickelberg, O.; Koenigshoff, M.; Bein, T.; Meiners, S. Protease-Mediated release of chemotherapeutics from mesoporous silica nanoparticles to ex vivo human and mouse lung tumors. *ACS Nano* **2015**, *9*, 2377–2389. [[CrossRef](#)]

31. Huang, X.; Yuan, Y.; Ruan, W.; Liu, L.; Liu, M.; Chen, S.; Zhou, X. PH-Responsive theranostic nanocomposites as synergistically enhancing positive and negative magnetic resonance imaging contrast agents. *J. Nanobiotechnol.* **2018**, *16*. [[CrossRef](#)] [[PubMed](#)]
32. Xia, L.; Guo, X.; Liu, T.; Xu, X.; Jiang, J.; Wang, F.; Cheng, Z.; Zhu, H.; Yang, Z. Multimodality imaging of naturally active melanin nanoparticles targeting somatostatin receptor subtype 2 in human small-cell lung cancer. *Nanoscale* **2019**, *11*, 14400–14409. [[CrossRef](#)] [[PubMed](#)]
33. Mir, T.A.; Yoon, J.-H.; Gurudatt, N.G.; Won, M.-S.; Shim, Y.-B. Ultrasensitive cytosensing based on an aptamer modified nanobiosensor with a bioconjugate: Detection of human non-small-cell lung cancer cells. *Biosens. Bioelectron.* **2015**, *74*, 594–600. [[CrossRef](#)] [[PubMed](#)]
34. Gao, F.; Cai, P.; Yang, W.; Xue, J.; Gao, L.; Liu, R.; Wang, Y.; Zhao, Y.; He, X.; Zhao, L.; et al. Ultrasmall Cu-64 Cu nanoclusters for targeting orthotopic lung tumors using accurate positron emission tomography imaging. *ACS Nano* **2015**, *9*, 4976–4986. [[CrossRef](#)]
35. Di Domenico, M.; Pozzi, D.; Palchetti, S.; Digiacomo, L.; Iorio, R.; Astarita, C.; Fiorelli, A.; Pierdiluca, M.; Santini, M.; Barbarino, M.; et al. Nanoparticle-Biomolecular corona: A new approach for the early detection of non-small-cell lung cancer. *J. Cell Physiol.* **2019**, *234*, 9378–9386. [[CrossRef](#)]
36. Card, J.W.; Zeldin, D.C.; Bonner, J.C.; Nestmann, E.R. Pulmonary applications and toxicity of engineered nanoparticles. *Am. J. Physiol. Lung.* **2008**, *295*, L400–L411. [[CrossRef](#)]
37. Jin, C.; Wang, K.; Oppong-Gyebi, A.; Hu, J. Application of nanotechnology in cancer diagnosis and therapy—A mini-review. *Int. J. Med. Sci.* **2020**, *17*, 2964–2973. [[CrossRef](#)]
38. Barabadi, H.; Vahidi, H.; Kamali, K.D.; Hosseini, O.; Mahjoub, M.A.; Rashedi, M.; Shoushtari, F.J.; Saravanan, M. Emerging theranostic gold nanomaterials to combat lung cancer: A systematic review. *J. Clust. Sci.* **2019**, *31*, 323–330. [[CrossRef](#)]
39. Hirsch, F.R.; Scagliotti, G.V.; Mulshine, J.L.; Kwon, R.; Curran, W.J.; Wu, Y.-L.; Paz-Ares, L. Lung cancer: Current therapies and new targeted treatments. *Lancet* **2017**, *389*, 299–311. [[CrossRef](#)]
40. Hussain, S. Nanomedicine for Treatment of Lung Cancer. *Adv. Exp. Med. Biol.* **2016**, *890*, 137–147. [[CrossRef](#)]
41. Madni, A.; Batool, A.; Noreen, S.; Maqbool, I.; Rehman, F.; Kashif, P.M.; Tahir, N.; Raza, A. Novel nanoparticulate systems for lung cancer therapy: An updated review. *J. Drug Target* **2017**, *25*, 499–512. [[CrossRef](#)] [[PubMed](#)]
42. Sim, A.J.; Kaza, E.; Singer, L.; Rosenberg, S.A. A review of the role of MRI in diagnosis and treatment of early stage lung cancer. *Clin. Transl. Radiat. Oncol.* **2020**, *24*, 16–22. [[CrossRef](#)] [[PubMed](#)]
43. Wild, J.M.; Marshall, H.; Bock, M.; Schad, L.R.; Jakob, P.M.; Puderbach, M.; Molinari, F.; Van Beek, E.J.R.; Biederer, J. MRI of the lung (1/3): Methods. *Insights Imaging* **2012**, *3*, 345–353. [[CrossRef](#)] [[PubMed](#)]
44. Bianchi, A.; Dufort, S.; Lux, F.; Fortin, P.-Y.; Tassali, N.; Tillement, O.; Coll, J.-L.; Cremillieux, Y. Targeting and in vivo imaging of non-small-cell lung cancer using nebulized multimodal contrast agents. *Proc. Natl. Acad. Sci. USA* **2014**, *111*, 9247–9252. [[CrossRef](#)]
45. Wang, L.; Lin, H.; Ma, L.; Jin, J.; Shen, T.; Wei, R.; Wang, X.; Ai, H.; Chen, Z.; Gao, J. Albumin-Based nanoparticles loaded with hydrophobic gadolinium chelates as T-1-T-2 dual-mode contrast agents for accurate liver tumor imaging. *Nanoscale* **2017**, *9*, 4516–4523. [[CrossRef](#)]
46. Li, F.; Zhi, D.; Luo, Y.; Zhang, J.; Nan, X.; Zhang, Y.; Zhou, W.; Qiu, B.; Wen, L.; Liang, G. Core/Shell Fe<sub>3</sub>O<sub>4</sub>/Gd<sub>2</sub>O<sub>3</sub> nanocubes as T-1-T-2 dual modal MRI contrast agents. *Nanoscale* **2016**, *8*, 12826–12833. [[CrossRef](#)]
47. Guldris, N.; Argibay, B.; Kolen'ko, Y.V.; Carbo-Argibay, E.; Sobrino, T.; Campos, F.; Salonen, L.M.; Banobre-Lopez, M.; Castillo, J.; Rivas, J. Influence of the separation procedure on the properties of magnetic nanoparticles: Gaining in vitro stability and T-1-T-2 magnetic resonance imaging performance. *J. Colloid Interface Sci.* **2016**, *472*, 229–236. [[CrossRef](#)]
48. Hermann, P.; Kotek, J.; Kubicek, V.; Lukes, I. Gadolinium(III) complexes as MRI contrast agents: Ligand design and properties of the complexes. *Dalton Trans.* **2008**, *23*, 3027–3047. [[CrossRef](#)]
49. Yoo, D.; Lee, J.-H.; Shin, T.-H.; Cheon, J. Theranostic magnetic nanoparticles. *Acc. Chem. Res.* **2011**, *44*, 863–874. [[CrossRef](#)]
50. Gao, W.; Wang, W.; Yao, S.; Wu, S.; Zhang, H.; Zhang, J.; Jing, F.; Mao, H.; Jin, Q.; Cong, H.; et al. Highly sensitive detection of multiple tumor markers for lung cancer using gold nanoparticle probes and microarrays. *Anal. Chim. Acta* **2017**, *958*, 77–84. [[CrossRef](#)]
51. Zhang, L.; Wang, J.; Zhang, J.; Liu, Y.; Wu, L.; Shen, J.; Zhang, Y.; Hu, Y.; Fan, Q.; Huang, W.; et al. Individual au-nanocube based plasmonic nanoprobe for cancer relevant MicroRNA biomarker detection. *ACS Sensors* **2017**, *2*, 1435–1440. [[CrossRef](#)] [[PubMed](#)]
52. Cheng, Z.; Zaki, A.A.; Hui, J.Z.; Muzykantov, V.R.; Tsourkas, A. Multifunctional nanoparticles: Cost versus benefit of adding targeting and imaging capabilities. *Science* **2012**, *338*, 903–910. [[CrossRef](#)] [[PubMed](#)]
53. Teramoto, A.; Yamada, A.; Tsukamoto, T.; Imaizumi, K.; Toyama, H.; Saito, K.; Fujita, H. Decision support system for lung cancer using PET/CT and microscopic images. *Adv. Exp. Med. Biol.* **2020**, *1213*, 73–94. [[CrossRef](#)] [[PubMed](#)]
54. Weissleder, R.; Nahrendorf, M.; Pittet, M.J. Imaging macrophages with nanoparticles. *Nat. Mater.* **2014**, *13*, 125–138. [[CrossRef](#)]
55. Thorsson, V.; Gibbs, D.L.; Brown, S.D.; Wolf, D.; Bortone, D.S.; Yang, T.-H.O.; Porta-Pardo, E.; Gao, G.F.; Plaisier, C.L.; Eddy, J.A.; et al. The immune landscape of cancer. *Immunity* **2018**, *48*, 812–830.e14. [[CrossRef](#)]
56. Sanhai, W.R.; Sakamoto, J.H.; Canady, R.; Ferrari, M. Seven challenges for nanomedicine. *Nat. Nanotechnol.* **2008**, *3*, 242–244. [[CrossRef](#)]
57. Kim, H.-Y.; Li, R.; Ng, T.S.C.; Courties, G.; Rodell, C.B.; Prytyskach, M.; Kohler, R.H.; Pittet, M.J.; Nahrendorf, M.; Weissleder, R.; et al. Quantitative imaging of tumor-associated macrophages and their response to therapy using cu-64-labeled macrin. *ACS Nano* **2018**, *12*, 12015–12029. [[CrossRef](#)]

58. Dufort, S.; Bianchi, A.; Henry, M.; Lux, F.; Duc, G.L.; Josserand, V.; Louis, C.; Perriat, P.; Cremillieux, Y.; Tillement, O.; et al. Nebulized gadolinium-based nanoparticles: A theranostic approach for lung tumor imaging and radiosensitization. *Small* **2015**, *11*, 215–221. [[CrossRef](#)]
59. Li, Z.; Tan, S.; Li, S.; Shen, Q.; Wang, K. Cancer drug delivery in the nano era: An overview and perspectives (Review). *Oncol. Rep.* **2017**, *38*, 611–624. [[CrossRef](#)]
60. Fu, L.; Wang, R.; Yin, L.; Shang, X.; Zhang, R.; Zhang, P. CYFRA21-1 tests in the diagnosis of non-small cell lung cancer: A meta-analysis. *Int. J. Biol. Markers* **2019**, *34*, 251–261. [[CrossRef](#)]
61. Roointan, A.; Ahmad Mir, T.; Ibrahim Wani, S.; Mati Ur, R.; Hussain, K.K.; Ahmed, B.; Abraham, S.; Savardashtaki, A.; Gandomani, G.; Gandomani, M.; et al. Early detection of lung cancer biomarkers through biosensor technology: A review. *J. Pharm. Biomed. Anal.* **2019**, *164*, 93–103. [[CrossRef](#)] [[PubMed](#)]
62. Hu, P.; Zhang, S.; Wu, T.; Ni, D.; Fan, W.; Zhu, Y.; Qian, R.; Shi, J. Fe-Au nanoparticle-coupling for ultrasensitive detections of circulating tumor DNA. *Adv. Mater.* **2018**, *30*. [[CrossRef](#)] [[PubMed](#)]
63. Djureinovic, D.; Hallstrom, B.M.; Horie, M.; Mattsson, J.S.M.; Fleur, L.L.; Fagerberg, L.; Brunnstrom, H.; Lindskog, C.; Madjar, K.; Rahnenfuehrer, J.; et al. Profiling cancer testis antigens in non-small-cell lung cancer. *JCI Insight*. **2016**, *1*. [[CrossRef](#)] [[PubMed](#)]
64. Jiang, Z.F.; Wang, M.; Xu, J.L. Thymidine kinase 1 combined with CEA, CYFRA21-1 and NSE improved its diagnostic value for lung cancer. *Life Sci.* **2018**, *194*, 1–6. [[CrossRef](#)]
65. Millares, L.; Barreiro, E.; Cortese, R.; Martinez-Romero, A.; Balcells, C.; Cascante, M.; Enguita, A.B.; Alvarez, C.; Rami-Porta, R.; Sanchez de Cos, J.; et al. Tumor-Associated metabolic and inflammatory responses in early stage non-small cell lung cancer: Local patterns and prognostic significance. *Lung Cancer* **2018**, *122*, 124–130. [[CrossRef](#)]
66. Maharjan, N.; Thapa, N.; Tu, J. Blood-Based biomarkers for early diagnosis of lung cancer: A review article. *JNMA J. Nepal. Med. Assoc.* **2020**, *58*, 519–524. [[CrossRef](#)]
67. Kalinke, L.; Thakrar, R.; Janes, S.M. The promises and challenges of early non-small cell lung cancer detection: Patient perceptions, low-dose CT screening, bronchoscopy and biomarkers. *Mol. Oncol.* **2020**. [[CrossRef](#)]
68. Saranya, G.; Joseph, M.M.; Karunakaran, V.; Nair, J.B.; Saritha, V.N.; Veena, V.S.; Sujathan, K.; Ajayaghosh, A.; Maiti, K.K. Enzyme-Driven switchable fluorescence-SERS diagnostic nanococktail for the multiplex detection of lung cancer biomarkers. *ACS Appl. Mater. Interfaces* **2018**, *10*, 38807–38818. [[CrossRef](#)]
69. Qiao, X.; Su, B.; Liu, C.; Song, Q.; Luo, D.; Mo, G.; Wang, T. Selective surface enhanced raman scattering for quantitative detection of lung cancer biomarkers in superparticle@MOF structure. *Adv. Mater.* **2018**, *30*. [[CrossRef](#)]
70. Liu, L.; Wu, S.; Jing, F.; Zhou, H.; Jia, C.; Li, G.; Cong, H.; Jin, Q.; Zhao, J. Bead-Based microarray immunoassay for lung cancer biomarkers using quantum dots as labels. *Biosens. Bioelectron.* **2016**, *80*, 300–306. [[CrossRef](#)]
71. Meng, X.; Chen, X.; Wu, W.; Zheng, W.; Deng, H.; Xu, L.; Chen, W.; Li, Z.; Peng, H. Electrochemiluminescent immunoassay for the lung cancer biomarker CYFRA21-1 using MoOx quantum dots. *Microchim. Acta* **2019**, *186*. [[CrossRef](#)] [[PubMed](#)]
72. Rakovich, T.Y.; Mahfoud, O.K.; Mohamed, B.M.; Prina-Mello, A.; Crosbie-Staunton, K.; Van den Broeck, T.; De Kimpe, L.; Sukhanova, A.; Baty, D.; Rakovich, A.; et al. Highly sensitive single domain antibody-quantum dot conjugates for detection of HER2 biomarker in lung and breast cancer cells. *ACS Nano* **2014**, *8*, 5682–5695. [[CrossRef](#)] [[PubMed](#)]
73. Zhang, H.; Ke, H.; Wang, Y.; Li, P.; Huang, C.; Jia, N. 3D carbon nanosphere and gold nanoparticle-based voltammetric cytosensor for cell line A549 and forearly diagnosis of non-small cell lung cancer cells. *Microchim. Acta* **2019**, *186*. [[CrossRef](#)]
74. Yang, T.; Guo, X.; Wu, Y.; Wang, H.; Fu, S.; Wen, Y.; Yang, H. Facile and label-free detection of lung cancer biomarker in urine by magnetically assisted surface-enhanced raman scattering. *ACS Appl. Mater. Interfaces* **2014**, *6*, 20985–20993. [[CrossRef](#)] [[PubMed](#)]
75. Bouillez, A.; Rajabi, H.; Jin, C.; Samur, M.; Tagde, A.; Alam, M.; Hiraki, M.; Maeda, T.; Hu, X.; Adeegbe, D.; et al. MUC1-C integrates PD-L1 induction with repression of immune effectors in non-small-cell lung cancer. *Oncogene* **2017**, *36*, 4037–4046. [[CrossRef](#)]
76. Wei, X.; Lai, Y.; Li, J.; Qin, L.; Xu, Y.; Zhao, R.; Li, B.; Lin, S.; Wang, S.; Wu, Q.; et al. PSCA and MUC1 in non-small-cell lung cancer as targets of chimeric antigen receptor T cells. *Oncoimmunology* **2017**, *6*. [[CrossRef](#)]
77. Qiao, L.-L.; Yao, W.-J.; Zhang, Z.-Q.; Yang, X.; Zhao, M.-X. The biological activity research of the nano-drugs based on 5-fluorouracil-modified quantum dots. *Int. J. Nanomed.* **2020**, *15*, 2765–2776. [[CrossRef](#)]
78. Zhao, M.-X.; Zeng, E.-Z.; Zhu, B.-J. The biological applications of inorganic nanoparticle drug carriers. *Chemnanomat* **2015**, *1*, 82–91. [[CrossRef](#)]
79. Ren, D.; Wang, B.; Hu, C.; You, Z. Quantum dot probes for cellular analysis. *Anal. Methods* **2017**, *9*, 2621–2632. [[CrossRef](#)]
80. Peng, H.; Jian, M.; Deng, H.; Wang, W.; Huang, Z.; Huang, K.; Liu, A.; Chen, W. Valence states effect on electrogenerated chemiluminescence of gold nanocluster. *ACS Appl. Mater. Interfaces* **2017**, *9*, 14929–14934. [[CrossRef](#)]
81. Even-Desrumeaux, K.; Nevoltris, D.; Lavaut, M.N.; Alim, K.; Borg, J.-P.; Audebert, S.; Kerfelec, B.; Baty, D.; Chames, P. Masked selection: A straightforward and flexible approach for the selection of binders against specific epitopes and differentially expressed proteins by phage display. *Mol. Cell. Proteomics* **2014**, *13*, 653–665. [[CrossRef](#)] [[PubMed](#)]
82. Li, C.; Tang, Z.; Hu, Z.; Wang, Y.; Yang, X.; Mo, F.; Lu, X. Natural single-domain antibody-nanobody: A novel concept in the antibody field. *J. Biomed. Nanotechnol.* **2018**, *14*, 1–19. [[CrossRef](#)] [[PubMed](#)]
83. Singh, R.D.; Shandilya, R.; Bhargava, A.; Kumar, R.; Tiwari, R.; Chaudhury, K.; Srivastava, R.K.; Goryacheva, I.Y.; Mishra, P.K. Quantum dot based nano-biosensors for detection of circulating cell free miRNAs in lung carcinogenesis: From biology to clinical translation. *Front Genet.* **2018**, *9*, 616. [[CrossRef](#)] [[PubMed](#)]

84. de la Torre, P.; Perez-Lorenzo, M.J.; Alcazar-Garrido, A.; Flores, A.I. Cell-Based nanoparticles delivery systems for targeted cancer therapy: Lessons from anti-angiogenesis treatments. *Molecules* **2020**, *25*. [[CrossRef](#)] [[PubMed](#)]
85. Song, Y.; Li, Z.; Guo, K.; Shao, T. Hierarchically ordered mesoporous carbon/graphene composites as supercapacitor electrode materials. *Nanoscale* **2016**, *8*, 15671–15680. [[CrossRef](#)] [[PubMed](#)]
86. Shoja, Y.; Kermanpur, A.; Karimzadeh, F. Diagnosis of EGFR exon21 L858R point mutation as lung cancer biomarker by electrochemical DNA biosensor based on reduced graphene oxide/functionalized ordered mesoporous carbon/Ni-oxytetracycline metallopolymer nanoparticles modified pencil graphite electrode. *Biosens. Bioelectron.* **2018**, *113*, 108–115. [[CrossRef](#)] [[PubMed](#)]
87. Aasi, A.; Aghaei, S.M.; Panchapakesan, B. A density functional theory study on the interaction of toluene with transition metal decorated carbon nanotubes: A promising platform for early detection of lung cancer from human breath. *Nanotechnology* **2020**, *31*, 415707. [[CrossRef](#)]
88. Wang, X.J.; Tian, L.F.; Du, H.; Li, M.; Mu, W.; Drinkwater, B.W.; Han, X.J.; Mann, S. Chemical communication in spatially organized protocell colonies and protocell/living cell micro-arrays. *Chem. Sci.* **2019**, *10*, 9446–9453. [[CrossRef](#)]
89. Wang, X.J.; Tian, L.F.; Ren, Y.S.; Zhao, Z.Y.; Du, H.; Zhang, Z.Z.; Drinkwater, B.W.; Mann, S.; Han, X.J. Chemical information exchange in organized protocells and natural cell assemblies with controllable spatial positions. *Small* **2020**, *16*. [[CrossRef](#)]
90. Zong, W.; Ma, S.H.; Zhang, X.N.; Wang, X.J.; Li, Q.C.; Han, X.J. A fissionable artificial eukaryote-like cell model. *J. Am. Chem. Soc.* **2017**, *139*, 9955–9960. [[CrossRef](#)]
91. Li, Q.C.; Li, S.B.; Zhang, X.X.; Xu, W.L.; Han, X.J. Programmed magnetic manipulation of vesicles into spatially coded prototissue architectures arrays. *Nat. Commun.* **2020**, *11*. [[CrossRef](#)] [[PubMed](#)]
92. Li, Q.C.; Han, X.J. Self-Assembled "breathing" grana-like cisternae stacks. *Adv. Mater.* **2018**, *30*. [[CrossRef](#)] [[PubMed](#)]
93. Li, Q.C.; Han, X.J. Self-Assembled rough endoplasmic reticulum-like proto-organelles. *Iscience* **2018**, *8*, 138–147. [[CrossRef](#)] [[PubMed](#)]
94. Wang, X.J.; Du, H.; Wang, Z.; Mu, W.; Han, X.J. Versatile phospholipid assemblies for functional synthetic cells and artificial tissues. *Adv. Mater.* **2020**. [[CrossRef](#)]
95. Wang, Y.; Fu, M.; Liu, J.; Yang, Y.; Yu, Y.; Li, J.; Pan, W.; Fan, L.; Li, G.; Li, X.; et al. Inhibition of tumor metastasis by targeted daunorubicin and dioscin codelivery liposomes modified with PFV for the treatment of non-small-cell lung cancer. *Int. J. Nanomed.* **2019**, *14*, 4071–4090. [[CrossRef](#)] [[PubMed](#)]
96. Adjei, I.M.; Sharma, B.; Labhassetwar, V. Nanoparticles: Cellular uptake and cytotoxicity. *Adv. Exp. Med. Biol.* **2014**, *811*, 73–91. [[CrossRef](#)]
97. Matczuk, M.; Ruzik, L.; Aleksenko, S.S.; Keppler, B.K.; Jarosz, M.; Timerbaev, A.R. Analytical methodology for studying cellular uptake, processing and localization of gold nanoparticles. *Anal. Chim. Acta* **2019**, *1052*, 1–9. [[CrossRef](#)]
98. Donahue, N.D.; Acar, H.; Wilhelm, S. Concepts of nanoparticle cellular uptake, intracellular trafficking, and kinetics in nanomedicine. *Adv. Drug Deliv. Rev.* **2019**, *143*, 68–96. [[CrossRef](#)]
99. Derk, R.; Davidson, D.C.; Manke, A.; Stueckle, T.A.; Rojanasakul, Y.; Wang, L. Potential in vitro model for testing the effect of exposure to nanoparticles on the lung alveolar epithelial barrier. *Sens. Biosensing. Res.* **2015**, *3*, 38–45. [[CrossRef](#)]
100. Wu, M.; Guo, H.; Liu, L.; Liu, Y.; Xie, L. Size-Dependent cellular uptake and localization profiles of silver nanoparticles. *Int. J. Nanomed.* **2019**, *14*, 4247–4259. [[CrossRef](#)]
101. Alkilany, A.M.; Murphy, C.J. Toxicity and cellular uptake of gold nanoparticles: What we have learned so far? *J. Nanopart. Res.* **2010**, *12*, 2313–2333. [[CrossRef](#)] [[PubMed](#)]
102. Zhou, W.; Cui, H.; Ying, L.; Yu, X.F. Enhanced cytosolic delivery and release of CRISPR/Cas9 by black phosphorus nanosheets for genome editing. *Angew. Chem. Int. Ed. Engl.* **2018**, *57*, 10268–10272. [[CrossRef](#)] [[PubMed](#)]
103. Peter, B.; Lagzi, I.; Teraji, S.; Nakanishi, H.; Cervenak, L.; Zambo, D.; Deak, A.; Molnar, K.; Truszka, M.; Szekacs, I.; et al. Interaction of positively charged gold nanoparticles with cancer cells monitored by an in situ label-free optical biosensor and transmission electron microscopy. *ACS Appl. Mater. Interfaces* **2018**, *10*, 26841–26850. [[CrossRef](#)] [[PubMed](#)]
104. Saadat, M.; Zahednezhad, F.; Zakeri-Milani, P.; Heidari, H.R.; Shahbazi-Mojarrad, J.; Valizadeh, H. Drug targeting strategies based on charge dependent uptake of nanoparticles into cancer cells. *J. Pharm. Pharm. Sci.* **2019**, *22*, 191–220. [[CrossRef](#)]